Mon. Not. R. Astron. Soc. **268**, 464–474 (1994)

The Parkes survey of methanol masers at 44.07 GHz

V. I. Slysh,[1] S. V. Kalenskii,[1] I. E. Val'tts[1] and R. Otrupcek[2]
[1] *Astro Space Center, Lebedev Physical Institute, Profsoyuznaya 84/32, 117810 Moscow, Russia*
[2] *Australia Telescope National Facility, CSIRO, PO Box 76, Epping, NSW 2121, Australia*

Accepted 1993 December 29. Received 1993 November 8

ABSTRACT

A survey of the Class I methanol masers in the transition 7_0–6_1 A^+ at 44.07 GHz has been carried out with the Parkes radio telescope. About 250 positions were searched in the direction of Galactic H II regions, H_2O masers and 6.7-GHz Class II methanol masers. 55 new methanol emission sources at 44 GHz were detected, amongst which is the second strongest in the sky, M8E, with a flux density of 520 Jy. Most of the newly found sources are associated with H_2O, OH and 6.7-GHz methanol masers and presumably are located in the common regions of star formation. A strong anticorrelation between Class I and II methanol masers was discovered. The nature of the anticorrelation is such that strong Class I masers do not co-exist with strong Class II masers and, where Class I and II masers co-exist, they have different radial velocities. The anticorrelation may be a consequence of the pumping radiation field acting on the population inversion, which is different for the two classes of masers. We suggest that the definitions of Class I and II methanol masers should be based solely on their transitions, and not by relating them to a particular type of associated astronomical object, as was originally proposed by Batrla et al. and Menten.

Key words: masers – stars: formation – ISM: molecules – radio lines: ISM.

1 INTRODUCTION

Following the initial discovery of methanol maser emission in the 7–6 A transition near 44 GHz by Morimoto, Ohishi & Kanzawa (1985) in Sgr B2, W51 and two other Galactic sources, extensive surveys have been carried out by Bachiller et al. (1990), Haschick, Menten & Baan (1990) and Kalenskii et al. (1992). Methanol masers at 44 GHz were found to be widespread and strong. Forster et al. (1990) also found 44-GHz methanol emission from 10 sources during their survey of molecules and masers near compact H II regions, although seven of them were common to the survey sources of either Haschick et al. (1990) or Bachiller et al. (1990). These Northern Hemisphere surveys have, to date, found a total of 54 methanol sources. To extend the search for 44-GHz methanol masers to cover the whole sky, we have carried out a survey of the southern sky with the Parkes radio telescope. In this survey 55 new methanol sources were discovered, doubling the total number of sources. With this number, statistical analysis becomes feasible and, as a result, improves the chances of understanding the nature of methanol masers emitting at 44 GHz. These are the so-called Class I masers, defined (vaguely) by Menten (1991a) as being 'offset from H II regions and OH masers'. Clearly, a more meaningful description of Class I masers could be made if a positive relation with certain astrophysical objects were found. In this paper, we present results of the Parkes survey, as well as some preliminary conclusions derived from the statistical analysis.

2 OBSERVATIONS

The observations were made over the period 1993 September 10–15, using the Parkes 64-m radio telescope. The rest frequency of the 7_0–$6_1 A^+$ methanol transition is 44.069 43 GHz, which is the highest frequency ever used for observations with the Parkes radio telescope. At this frequency the inner 16-m diameter central section of the telescope was illuminated. This section has a surface error of 0.27 cm (rms), resulting in an aperture efficiency of 34 per cent, a half-power beamwidth of 1.6 arcmin, and a sensitivity of 39.4 Jy K^{-1}. The pointing accuracy was better than 15 arcsec (rms). A reflection-wave maser amplifier receiver with single-sideband input noise temperature 52 K was used. This receiver was based on the concept devised by Moore & Neff (1982); the system noise temperature varied between 125 and

Table 1. 44-GHz methanol masers detected.

Source (l, b)	RA (1950) h m s	Dec (1950) ° ′ ″	LSR radial velocity (km s^{-1})	Line width (km s^{-1})	Area (Jy km s^{-1})
269.20 -1.13	09 01 52.96	-48 16 07.1	9.44 (.01)	0.31 (.03)	7.2 (.05)
270.26 +0.84	09 14 52.26	-47 43 34.1	8.56 (.01)	0.23 (.02)	3.3 (.04)
			9.71 (.02)	0.30 (.05)	11.1 (1.9)
			10.41 (.11)	1.75 (.25)	20.7 (2.6)
294.97 -1.73	11 36 51.54	-63 12 09.4	-8.25 (.07)	0.85 (.16)	10.4 (1.7)
300.97 +1.14	12 32 00.78	-61 23 30.2	-42.21 (.01)	0.49 (.03)	19.3 (1.0)
301.14 -0.23	12 32 41.18	-62 46 07.2	-36.36 (.02)	0.69 (.03)	28.0 (1.4)
			-35.34 (.01)	0.68 (.03)	34.7 (1.6)
305.21 +0.21	13 07 57.54	-62 18 44.2	-42.34 (.008)	0.49 (.02)	37.1 (1.8)
			-40.82 (.16)	2.16 (.29)	23.8 (3.3)
305.36 +0.20	13 09 21.00	-62 17 30.0	-40.33 (.008)	0.20 (.02)	3.9 (0.4)
			-34.77 (.01)	0.37 (.02)	9.1 (0.7)
			-33.69 (.01)	0.40 (.03)	31.2 (2.9)
			-33.13 (.03)	0.56 (.06)	59.4 (5.0)
316.76 -0.02	14 41 07.81	-59 35 33.1	-39.30 (.02)	0.36 (.03)	9.7 (.08)
318.05 +0.09	14 49 52.91	-58 56 47.1	-49.51 (.03)	0.50 (.07)	16.8 (2.1)
			-48.91 (.03)	0.49 (.07)	13.8 (2.0)
318.94 -0.20	14 57 01.50	-58 47 14.2	-36.10 (.01)	0.33 (.03)	8.3 (0.7)
			-35.60 (.03)	0.28 (.06)	3.1 (0.6)
320.28 -0.31	15 06 25.71	-58 14 02.2	-66.30 (.03)	0.94 (.07)	42.7 (3.0)
			-65.05 (.05)	0.65 (.12)	15.0 (2.5)
322.17 +0.62	15 14 50.20	-56 27 51.1	-53.92 (.02)	0.27 (.05)	7.8 (1.2)
			-58.50 (.03)	0.33 (.07)	8.6 (1.5)
323.74 -0.27	15 27 52.41	-56 20 48.1	-50.51 (.03)	0.78 (.17)	9.8 (5.0)
			-49.90 (.03)	0.35 (.06)	8.1 (1.5)
324.72 +0.34	15 31 06.71	-55 17 28.1	-51.84 (.02)	0.41 (.04)	17.5 (1.5)
326.66 +0.57	15 40 59.00	-53 57 24.1	-41.23 (.06)	1.35 (.13)	15.9 (1.3)
327.29 -0.58	15 49 13.01	-54 28 12.1	-54.27 (.01)	0.11 (.03)	2.0 (0.4)
			-46.49 (.02)	0.73 (.04)	19.4 (1.6)
			-45.51 (.02)	0.37 (.05)	8.4 (1.2)
			-44.31 (.05)	0.87 (.11)	22.7 (2.7)
328.20 -0.58	15 54 02.31	-53 53 37.1	-40.79 (.02)	0.58 (.05)	13.2 (0.9)
328.24 -0.55	15 54 06.12	-53 50 47.1	-47.50 (.02)	0.16 (.03)	1.5 (0.4)
			-41.11 (.02)	0.32 (.05)	3.8 (0.7)
328.81 +0.64	15 52 00.01	-52 34 03.9	-42.43 (.03)	1.24 (.06)	48.4 (2.0)
			-40.61 (.05)	1.15 (.04)	27.0 (2.1)
329.03 -0.21	15 56 42.01	-53 04 22.1	-47.04 (.01)	0.15 (.04)	6.1 (1.6)
			-46.66 (.04)	1.12 (.14)	39.5 (1.5)
			-43.65 (.04)	0.68 (.19)	16.9 (2.4)
331.13 -0.25	16 07 11.01	-51 42 53.1	-91.00 (.02)	0.70 (.04)	66.5 (3.1)
			-88.37 (.03)	0.62 (.06)	24.9 (2.6)
			-87.36 (.03)	0.43 (.08)	8.4 (1.9)
			-84.60 (.07)	0.38 (.15)	11.6 (4.3)
331.34 -0.35	16 08 37.41	-51 38 32.1	-65.69 (.03)	0.40 (.09)	9.6 (2.2)
			-65.38 (.03)	0.24 (.05)	7.0 (1.3)
333.13 -0.43	16 17 13.01	-50 28 18.1	-51.33 (.02)	0.48 (.14)	7.6 (0.3)
			-49.92 (.06)	0.85 (.21)	81.6 (7.5)
			-49.00 (.08)	0.44 (.08)	33.8(18.3)
333.13 -0.43	16 17 13.01	-50 28 18.1	-51.33 (.02)	0.48 (.14)	7.6 (0.3)
			-49.92 (.06)	0.85 (.21)	81.6 (7.5)
			-49.00 (.08)	0.44 (.08)	33.8(18.3)
			-48.23 (.05)	0.81 (.11)	79.8 (3.1)
			-47.41 (.04)	0.46 (.10)	20.7(10.3)
			-47.69 (.06)	0.68 (.08)	23.4(15.3)
			-45.78 (.20)	0.67 (.23)	8.5 (4.2)
333.23 -0.05	16 16 02.1	-50 07 50.1	-87.24 (.01)	1.33 (.01)	272.7 (8.8)
			-87.15 (.01)	0.47 (.01)	59.9 (8.9)
			-85.41 (.04)	0.33 (.04)	8.1 (2.3)
333.61 -0.22	16 18 25.01	-49 59 08.1	-49.34 (.08)	0.61 (.08)	12.9 (1.5)
335.59 -0.29	16 27 15.40	-48 37 20.1	-45.43 (.02)	0.55 (.02)	87.0 (2.5)

Table 1 – *continued*

Source (l, b)	RA (1950) h m s	Dec (1950) ° ' "	LSR radial velocity (km s^{-1})	Line width (km s^{-1})	Area (Jy km s^{-1})
335.78 +0.17	16 26 03.00	-48 09 44.1	-50.03 (.08)	1.28 (.08)	17.2 (1.5)
			-48.53 (.10)	0.82 (.10)	18.0 (2.0)
336.41 -0.26	16 30 31.51	-48 00 08.1	-87.57 (.06)	0.72 (.06)	37.0 (2.7)
337.40 -0.41	16 35 08.01	-47 22 23.1	-44.17 (.02)	0.55 (.02)	22.4 (0.8)
			-42.28 (.02)	0.22 (.02)	5.9 (0.5)
337.91 -0.47	16 37 27.01	-47 02 10.1	-43.44 (.003)	0.40 (.006)	109.3 (1.6)
338.92 +0.56	16 36 54.01	-45 36 05.0	-62.92 (.008)	0.50 (.02)	83.3 (2.7)
			-62.36 (.01)	0.37 (.03)	30.2 (1.7)
			-60.35 (.01)	0.38 (.03)	31.5 (3.5)
			-59.68 (.02)	0.73 (.04)	65.4 (3.9)
339.88 -1.26	16 48 24.76	-46 03 34.0	-31.87 (.06)	0.76 (.14)	5.5 (0.9)
341.19 -0.22	16 48 39.50	-44 23 33.5	-41.91 (.005)	0.31 (.01)	28.8 (0.9)
341.22 -0.21	16 48 42.10	-44 21 53.0	-45.66 (.04)	0.35 (.06)	1.9 (0.3)
			-44.51 (.07)	1.08 (.08)	16.6 (0.8)
			-43.77 (.03)	0.44 (.06)	11.2 (3.0)
			-43.05 (.07)	0.77 (.16)	19.0 (3.8)
			-41.86 (.08)	1.01 (.34)	7.0 (2.0)
343.12 -0.06	16 54 43.00	-42 47 49.00	-32.76 (.01)	0.95 (.03)	68.3 (2.1)
			-31.50 (.01)	0.66 (.05)	35.4 (2.1)
			-30.41 (.04)	1.08 (.06)	41.1 (1.9)
			-28.66 (.04)	0.45 (.08)	4.9 (0.8)
			-27.29 (.01)	0.52 (.02)	48.3 (2.0)
344.23 -0.57	17 00 35.16	-42 14 29.7	-23.97 (.003)	0.23 (.008)	2.5 (0.1)
			-22.44 (.03)	1.20 (.08)	9.4 (0.8)
			-21.13 (.03)	0.28 (.05)	3.9 (0.8)
			-20.31 (.08)	0.62 (.19)	30.0 (6.0)
345.00-0.22	17 01 38.51	-41 24 59.0	-28.77 (.01)	0.58 (.03)	15.3 (0.8)
			-27.88 (.06)	0.61 (.12)	42.3 (7.0)
345.01 +1.79	16 53 21.00	-40 09 40.0	-13.31 (.05)	1.35 (.20)	10.5 (2.6)
			-13.16 (.04)	0.41 (.07)	13.7 (1.9)
345.41 -0.94	17 06 02.01	-41 31 44.0	-22.86 (.06)	0.78 (.13)	9.1 (1.3)
345.51 +0.35	17 00 54.00	-40 40 02.0	-17.42 (.03)	0.35 (.04)	2.4 (0.4)
			-16.52 (.03)	0.61 (.14)	9.9 (1.0)
			-14.68 (.09)	0.45 (.13)	3.5 (1.7)
348.18 -0.49	17 08 39.01	-38 27 06.0	-7.18 (.01)	0.22 (.02)	8.8 (0.8)
			-6.61 (.009)	0.39 (.02)	4.7 (0.3)
			-5.87 (.10)	0.24 (.23)	4.9 (2.8)
349.10 +0.11	17 13 01.00	-37 56 06.0	-77.98 (.01)	0.34 (.03)	8.1 (0.7)
351.16 +0.70	17 16 35.51	-35 54 44.0	-7.92 (.01)	0.33 (.01)	21.3 (1.3)
			-7.53 (.02)	0.25 (.004)	8.1 (1.0)
			-7.05 (.005)	0.58 (.06)	41.8 (1.5)
			-6.48 (.02)	0.35 (.01)	20.6 (2.8)
			-6.15 (.01)	0.25 (.02)	9.7 (5.0)
			-5.87 (.02)	0.68 (.19)	27.4 (1.0)
			-4.51 (.07)	0.35 (.05)	12.9 (3.6)
351.24 +0.67	17 16 54.51	-35 51 58.0	-4.52 (.007)	0.34 (.02)	7.3 (0.3)
			-4.04 (.007)	0.37 (.01)	14.9 (0.5)
			-3.47 (.02)	0.41 (.02)	36.2 (3.7)
			-2.47 (.03)	0.34 (.04)	8.5 (1.0)
			-0.58 (.04)	0.26 (.07)	5.1 (1.5)
351.41 +0.64	17 17 32.35	-35 44 04.2	-8.39 (.02)	1.40 (.03)	55.8 (2.7)
			-7.94 (.01)	0.26 (.02)	9.7 (1.7)
			-7.02 (.006)	0.27 (.01)	7.8 (0.5)
			-6.32 (.02)	0.49 (.05)	17.6 (1.6)
			-4.81 (.04)	0.24 (.09)	4.2 (1.5)
351.64 -1.26	17 25 55.00	-36 37 48.0	-16.21 (.02)	0.21 (.02)	3.5 (0.6)
			-13.05 (.02)	1.21 (.04)	15.4 (0.1)
			-12.52 (.24)	0.36 (.20)	5.6 (3.1)
351.78 -0.54	17 23 20.67	-36 06 45.4	-8.26 (.008)	0.43 (.02)	20.6 (0.7)
			-7.41 (.01)	0.39 (.03)	28.2 (1.8)

Table 1 – *continued*

Source (l, b)	RA (1950) h m s	Dec (1950) ° ' "	LSR radial velocity (km s^{-1})	Line width (km s^{-1})	Area (Jy km s^{-1})
			-6.90 (.006)	0.41 (.01)	61.8 (1.9)
			-2.30 (.01)	0.42 (.03)	47.4 (2.5)
353.41 -0.36	17 27 07.00	-34 39 41.00	-18.84 (.02)	0.44 (.04)	5.1 (0.5)
			-16.47 (.05)	0.64 (.10)	20.1 (2.3)
354.61 +0.47	17 27 00.00	-33 11 38.0	-21.29 (.006)	0.40 (.01)	4.0 (0.2)
			-17.80 (.07)	0.49 (.16)	27.2 (5.6)
359.62 -0.25	17 42 30.00	-29 22 31.0	18.12 (.009)	1.09 (.02)	20.1 (0.5)
			19.37 (.01)	0.36 (.03)	38.1 (1.9)
			20.58 (.07)	1.07 (.17)	32.5 (3.5)
0.54 -0.85	17 47 04.10	-28 54 01.0	14.80 (.02)	0.65 (.04)	22.0 (1.1)
6.05 -1.45	18 01 49.71	-24 26 56.0	10.55 (.009)	0.37 (.03)	37.3 (0.7)
			10.82 (.02)	0.32 (.05)	166.1(11.1)
			11.13 (.10)	0.28 (.04)	95.3(21.9)
12.89 +0.49	18 08 56.40	-17 32 14.0	31.44 (.01)	0.32 (.03)	7.8 (0.7)
14.33 -0.64	18 16 00.80	-16 49 06.0	19.08 (.007)	0.59 (.02)	42.6 (1.2)
			20.38 (.01)	0.65 (.02)	30.4 (1.5)
			22.55 (.01)	0.80 (.03)	69.3 (2.9)
			23.46 (.02)	0.45 (.05)	54.0 (4.4)
16.59-0.06	18 18 20.30	-14 33 18.0	61.17 (.09)	1.02 (.15)	9.5 (1.8)
			61.18 (.04)	0.16 (.07)	2.0 (1.6)
23.01 -0.41	18 31 56.70	-09 03 18.0	77.12 (.01)	0.32 (.03)	10.3 (0.9)
23.43 -0.19	18 31 55.80	-08 34 17.0	96.74 (.006)	0.69 (.02)	26.3 (0.6)
			97.69 (.01)	0.43 (.02)	5.2 (0.2)
			99.68 (.02)	0.38 (.03)	30.0 (2.3)
			101.21 (.01)	0.29 (.02)	13.0 (1.1)
			102.35 (.10)	1.33 (.23)	59.9 (9.4)
30.69 -0.06	18 44 58.9	-02 04 27.0	85.43 (.02)	0.35 (.04)	5.1 (0.7)
			89.50 (.09)	0.48 (.21)	14.3 (3.7)

300 K, depending on elevation and weather conditions. The spectrometer was a digital autocorrelator with 2048 channels and 16-MHz bandwidth, giving a velocity resolution of 0.053 km s^{-1}. The observations were performed in the frequency-switching mode. The data were corrected for atmospheric absorption by using measured system-noise temperatures.

3 RESULTS

Our source list consisted of Galactic H II regions, including those showing absorption in the 12-GHz methanol line (Peng & Whiteoak 1992), H_2O masers, 6.7-GHz Class II methanol masers and dark clouds. In total, ~250 sources were observed. Emission was detected toward 55 new sources, and some previously known sources were reobserved. Line parameters determined from Gaussian fits are given in Table 1, and the observed spectra are plotted in Figs 1–4. For a number of sources, a limited grid of points was observed to determine the source position, and we give the new positions in Table 1. Sources toward which no emission was detected are listed in Table 2, where a typical upper limit on the flux density is between 5 and 10 Jy, depending on integration time and weather conditions. One of the sources from Table 2, 11.93 − 0.62, was listed by Bachiller et al. (1990) as a positive detection. Bachiller et al. (1990) found a narrow feature at 35.19 km s^{-1} superimposed on a broad plateau. We could not see any narrow feature with a flux density in excess of 5 Jy, although it is possible that the broad plateau may be present in our spectrum. In the detection list we have included three sources which were observed by Forster et al. (1990) and Haschick et al. (1990), since our spectra differ significantly (see Section 4). Four source positions in the Large Magellanic Cloud were observed, but no emission lines were detected.

4 DISCUSSION

4.1 Notes on selected sources

333.13 − 0.43. The 44-GHz methanol profile consists of six or seven features regularly spaced in radial velocity (Fig. 2h), with velocity separation of ~0.8 km s^{-1}. The profile of the associated H_2O maser (Batchelor et al. 1980) shows only three spectral features within roughly the same velocity interval, and there is a small H II region. The 6.7-GHz methanol maser has three spectral features at the overlapping radial velocities (MacLeod & Gaylard 1992).

333.23 − 0.05 (Fig. 2i). This is one of the strongest new 44-GHz methanol masers. It has a triangular-shaped profile with a peak at a radial velocity of −87.2 km s^{-1}. It is associated with a small H II region (Haynes, Caswell & Simons 1978), OH and H_2O masers (Batchelor et al. 1980; Caswell, Haynes & Goss 1980). The H_2O profile has a similar shape to that of 44-GHz methanol, and is at the same radial velocity.

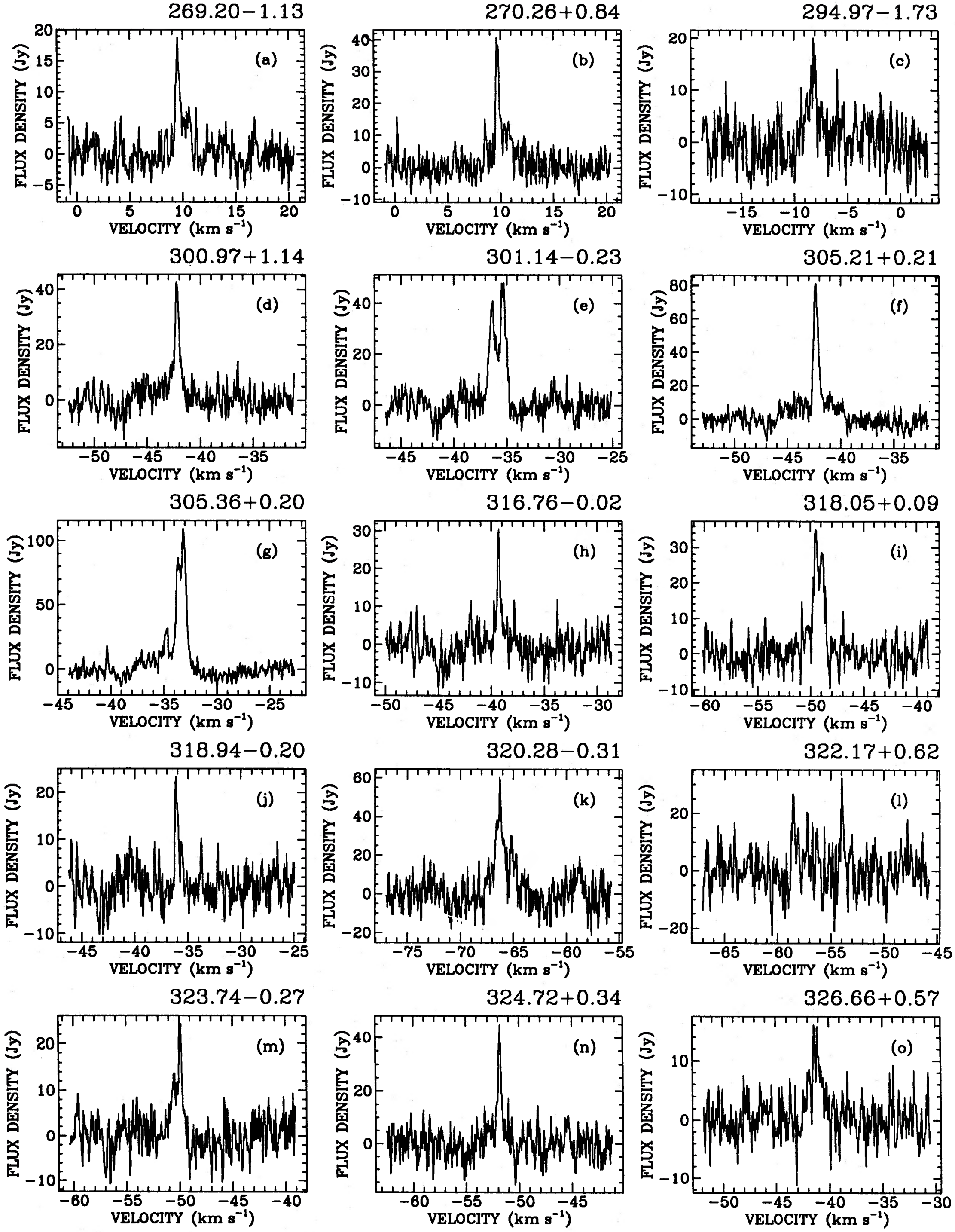

Figure 1. Spectra of 44-GHz methanol emission sources in the Galactic longitude interval $l=269°–327°$. The velocity resolution is 0.053 km s^{-1}.

335.59−0.29 (Fig. 2k). This strong source has only one narrow component at -45.4 km s^{-1}, while in the 6.7-GHz methanol spectrum there are four components at more negative velocities (MacLeod & Gaylard 1992).

337.91−0.47 (Fig. 2o). This is another very strong 44-GHz source with a single narrow feature at -43.4 km s^{-1}. The H_2O spectrum is more complicated, with additional features (Batchelor et al. 1980). The 6.7-GHz methanol spectrum consists of two closely spaced narrow lines, shifted from the 44-GHz line velocity to the positive side (MacLeod & Gaylard 1992). There is a rather strong, compact H II region associated with this maser (Haynes et al. 1978).

341.22−0.21 (Fig. 3d). This is one of several quasi-thermal sources showing a weak wide line. The 6.7-GHz spectrum consists of a pair of narrow lines on both sides of the 44-GHz line velocity (MacLeod, Gaylard & Nicolson 1992).

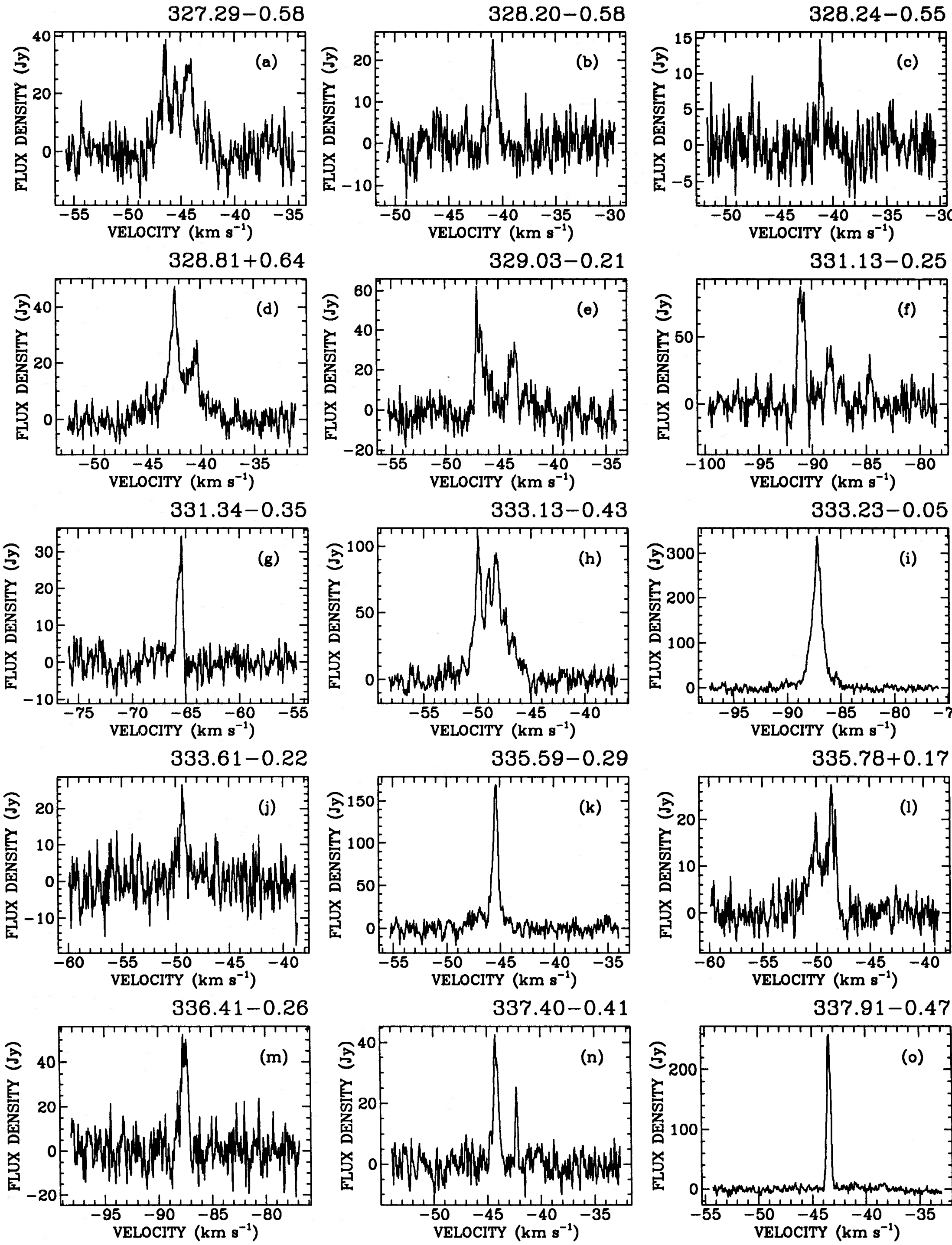

Figure 2. As Fig. 1, for $l = 327°–338°$.

Other examples of such quasi-thermal sources are 326.66 + 0.57 (Fig. 1o), and 328.20 − 0.58 (Fig. 2b). For the latter source there is some evidence that it is extended by our beam, since a similar line was observed 1.8 arcmin away. At this position Peng & Whiteoak (1992) found methanol absorption at 12 GHz.

343.12 − 0.06 (Fig. 3e). There are four or more narrow spectral components in the profile of this source. The source is displaced from a nearby H II region, but is associated with OH and H_2O masers. The H_2O profile also reveals many components within the same velocity interval (Batchelor et al. 1980). No Class II masers were reported at this position.

351.16 + 0.70 (NGC 6334B), 351.24 + 0.67 (NGC 6334C). These are two more strong 44-GHz masers in the NGC 6334 region, in addition to the two detected by Haschick et al. (1990). The spectrum of NGC 6334B is

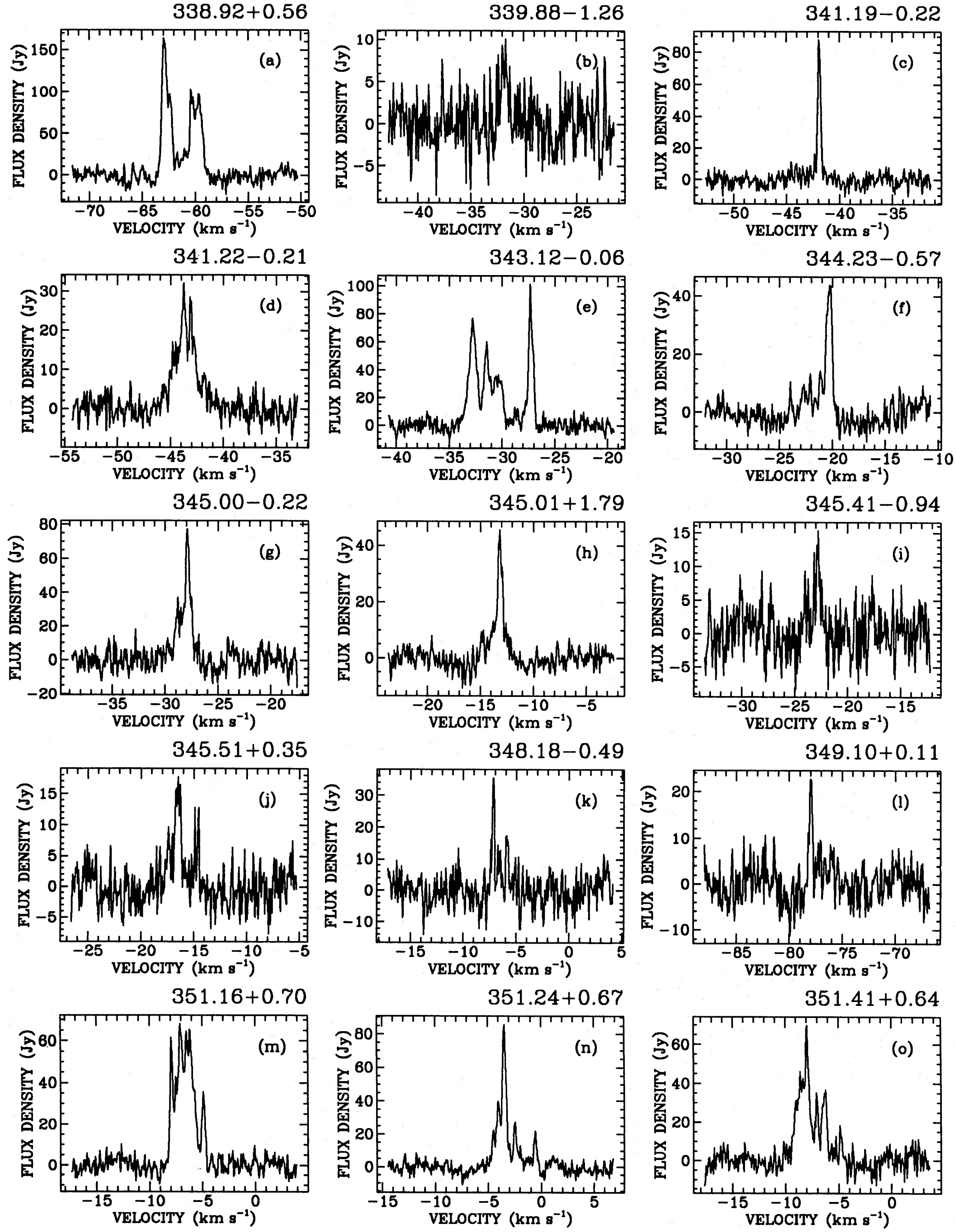

Figure 3. As Fig. 1, for $l = 338°–351\overset{\circ}{.}41$.

rather wide, but rippled, and might be an overlap of many narrow features (Fig. 3m). The 6.7-GHz methanol maser was found by Menten (1991b). NGC 6334C coincides with the HH object GGD 25. Its profile also has multiple components (Fig. 3n). In 6.7- and 12-GHz methanol transitions it is seen in absorption within the same radial velocity interval (Menten 1991b; Peng & Whiteoak 1992).

351.41 + 0.64 (NGC 6334F) and *351.78 − 0.54.* These two sources were detected at 44 GHz by Forster et al. (1990), and NGC 6334F was also observed by Haschick et al. (1990). We found a complex profile of NGC 6334F with five narrow features (Fig. 3o), in contrast to Forster et al. (1990) and Haschick et al. (1990) who reported a single broad feature. In 351.78 − 0.54 we found four narrow components

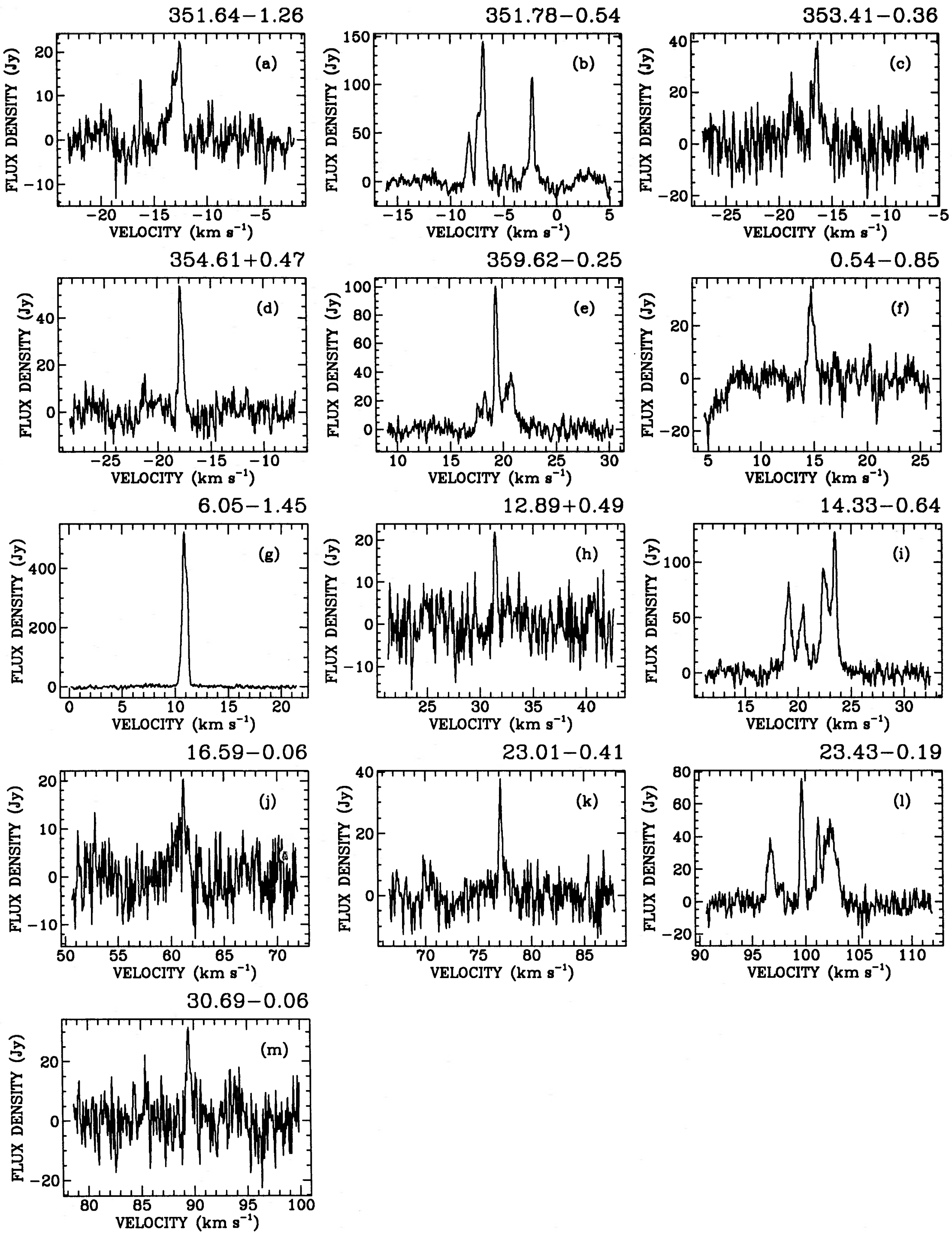

Figure 4. As Fig. 1, for $l = 351\overset{\circ}{.}64$–$30\overset{\circ}{.}69$.

(Fig. 4b), while Forster et al. reported only one broad Gaussian feature.

0.54−0.85 (RCW 142). 44-GHz emission from this source was detected by Forster et al., but again our profile is different from theirs. We see a single narrow (0.65 km s^{-1}) line at 14.8 km s^{-1} (Fig. 4f), while Forster et al. give Gaussian parameters of a broad (6.1 km s^{-1}) line at 17.2 km s^{-1}.

6.05−1.45 (M8E). This is the strongest source in our sample, and the second strongest yet found at 44 GHz, with a peak flux density of more than 500 Jy. As a methanol maser, it was first detected in 4_{-1}–3_0 E transition at 36 GHz in Puschino (Kalenskii et al. 1993). Its asymmetric narrow line may consist of two components (Fig. 4g). There is an H_2O maser at this position (Lada et al. 1976), but no 6.7-GHz methanol source has been reported.

14.33−0.64 (Fig. 4i). This is a strong source with four

Table 2. Sources undetected at 44-GHz.

Source (l, b)	RA (1950) h	m	s	Dec (1950) °	′	″	LSR radial velocity [a] (km s^{-1})
175.84 -21.48	04	16	08.98	+19	17	54.9	0.0
176.23 -20.87	04	19	06.98	+19	25	44.9	0.0
LMC N105	05	10	12.64	-68	57	07.8	251.0 (b)
LMC N113	05	13	43.43	-69	25	55.8	251.0 (b)
210.42 -19.76	05	33	53.17	-06	46	49.9	10.0
LMC N157	05	39	09.13	-69	06	09.8	251.0 (b)
LMC N160	05	40	08.33	-69	39	53.8	251.0 (b)
205.45 -14.55	05	43	35.87	-00	09	25.9	10.0
213.83 +0.62	06	52	43.57	-00	27	11.0	10.0
232.62 +1.00	07	29	54.97	-16	51	47.0	23.0
233.76 -0.19	07	27	52.67	-18	26	08.0	43.0
243.16 +0.37	07	50	18.37	-26	17	53.0	52.0
254.66 +0.21	08	18	54.06	-36	03	00.0	64.0
263.25 +0.52	08	47	00.46	-42	43	15.0	13.0
264.29 +1.47	08	54	38.46	-42	54	06.0	5.0
265.14 1.45	08	57	35.86	-43	33	30.0	7.2
267.94 -1.06	08	57	21.86	-47	18	59.0	-1.0
268.43 -0.85	09	00	13.96	-47	32	36.1	2.3
269.11 -1.12	09	01	44.96	-48	14	00.1	4.3
274.01 -1.14	09	22	49.26	-51	46	38.6	39.3
281.17 -1.64	09	57	49.26	-56	49	20.1	0.0
281.56 -2.48	09	56	23.06	-57	43	25.1	0.0
281.59 -0.97	10	03	11.56	-56	32	01.1	-5.2
282.03 -1.18	10	04	53.76	-56	57	40.1	-5.2
283.14 -1.01	10	12	22.26	-57	27	16.1	0.0
284.30 -0.34	10	22	19.96	-57	32	00.1	7.0
284.35 -0.42	10	22	21.56	-57	37	29.2	7.0
285.26 -0.05	10	29	36.96	-57	46	49.1	3.0
286.39 -1.35	10	32	04.86	-59	28	24.1	38.0
287.39 -0.63	10	41	38.96	-59	19	42.2	-24.6
289.88 -0.80	10	58	56.86	-60	34	19.2	22.0
290.37 +1.66	11	10	07.37	-58	30	00.2	-21.0
291.27 -0.72	11	09	41.47	-61	02	29.2	-88.0
291.57 -0.43	11	12	52.07	-60	53	02.2	11.0
291.61 -0.53	11	12	54.47	-60	59	36.2	12.2
291.64 -0.55	11	13	04.77	-61	01	07.2	1.2
291.65 -0.60	11	13	01.37	-61	04	07.2	14.0
291.87 -0.68	11	14	23.67	-61	13	36.2	25.0
294.51 -1.62	11	33	12.87	-62	58	15.2	-12.0
295.00 -1.74	11	37	04.77	-63	13	29.2	-13.0
297.66 -0.97	12	01	33.58	-63	04	53.2	24.0
298.18 -0.79	12	06	22.97	-62	59	14.2	31.0
298.22 -0.34	12	07	19.88	-62	32	56.2	31.8
298.26 +0.74	12	09	07.97	-61	29	37.2	25.0
299.01 +0.13	12	14	42.08	-62	12	19.2	19.0
300.50 -0.18	12	27	13.98	-62	40	19.2	8.0
301.12 +0.97	12	33	09.49	-61	34	23.4	-3.0
302.02 -0.08	12	40	29.49	-62	39	39.2	-35.0
304.95 +0.53	13	05	37.59	-62	00	26.8	-30.0
305.10 +0.14	13	07	06.78	-62	23	17.2	-38.0
305.36 +0.15	13	09	22.59	-62	21	27.2	-37.0
305.80 -0.24	13	13	26.69	-62	42	43.2	-30.0
308.92 +0.12	13	39	33.19	-61	53	59.2	-54.0
309.17 -1.12	13	43	53.30	-63	03	27.2	-50.5
309.90 -0.37	13	47	15.79	-61	26	43.8	-53.0
309.93 +0.48	13	47	14.70	-61	20	25.2	-70.5
311.63 +0.29	14	01	18.20	-61	05	45.2	-37.3
311.64 -0.38	14	02	59.30	-61	44	06.2	33.0
311.89 +0.10	14	03	52.90	-61	12	14.1	-50.0
311.92 +0.23	14	03	48.30	-61	04	18.6	-51.0
311.95 +0.14	14	04	12.40	-61	09	05.2	-42.0
312.60 +0.04	14	09	35.30	-61	03	20.2	-63.0
313.35 +0.23	14	14	59.10	-60	38	12.2	-4.0
313.78 -0.89	14	21	25.00	-61	32	27.2	-50.0
314.25 +0.11	14	22	14.20	-60	26	47.2	-45.0
316.37 -0.37	14	39	26.30	-60	04	32.1	-3.0
316.64 -0.09	14	40	29.11	-59	42	46.2	-18.0
316.80 -0.06	14	41	32.40	-59	37	21.2	-37.3
318.91 -0.18	14	56	45.11	-58	47	14.8	-29.0
319.16 -0.42	14	59	19.11	-58	53	02.2	-22.0

Table 2 – *continued*

Source (l, b)	RA (1950) h	m	s	Dec (1950) °	′	″	LSR radial velocity [a] (km s^{-1})
319.38 -0.03	14	59	21.51	-58	25	40.7	-14.0
319.83 -0.20	15	03	00.41	-58	21	30.1	-5.0
320.15 +0.78	15	01	32.20	-57	21	02.3	-36.0
320.23 -0.29	15	05	59.60	-58	14	18.2	-54.0
320.25 -0.31	15	06	13.30	-58	14	49.1	-68.0
320.31 +1.06	15	01	32.20	-57	01	32.4	-36.0
320.32 -0.21	15	06	15.20	-58	07	43.6	-11.0
321.04 -0.52	15	12	08.91	-58	01	44.1	-61.0
321.14 -0.53	15	12	50.91	-57	59	06.1	-64.0
321.71 +1.16	15	10	01.20	-56	14	47.5	-32.0
323.46 -0.09	15	25	27.81	-56	21	24.1	-67.5
324.20 +0.12	15	29	00.51	-55	46	09.1	-93.0
326.44 +0.91	15	38	24.51	-53	48	50.4	-39.0
326.77 -0.26	15	45	04.11	-54	32	40.1	-58.0
327.12 +0.51	15	43	43.01	-53	43	48.1	-84.0
327.39 +0.44	15	45	27.01	-53	36	25.1	-79.0
327.76 -0.35	15	50	45.01	-53	59	59.1	-72.0
327.99 -0.09	15	50	48.11	-53	39	03.1	-45.0
328.25 -0.53	15	54	07.57	-53	49	25.1	-45.0
328.30 +0.43	15	50	15.01	-53	02	46.1	-96.0
328.59 -0.52	15	55	48.91	-53	35	42.3	-51.0
329.40 -0.46	15	59	41.00	-53	01	33.1	-76.0
330.31 -0.39	16	03	49.00	-52	22	11.1	-76.0
330.88 -0.37	16	06	30.01	-51	58	14.1	-56.0
330.95 -0.19	16	06	03.00	-51	47	30.1	-88.0
331.28 -0.18	16	07	36.01	-51	33	40.1	-92.1
331.38 +0.01	16	07	13.80	-51	21	11.1	-81.0
331.51 -0.10	16	08	21.00	-51	21	11.1	-95.0
331.54 -0.07	16	08	22.71	-51	18	10.1	-84.0
331.56 -0.13	16	08	40.40	-51	20	05.1	-104.0
332.15 -0.45	16	12	49.81	-51	09	52.1	-55.0
332.65 -0.63	16	15	56.00	-50	56	48.1	-44.0
332.72 -0.62	16	16	14.21	-50	53	18.1	-46.0
332.83 -0.55	16	16	24.01	-50	45	46.1	-70.8
333.03 -0.45	16	16	52.01	-50	33	12.1	-54.5
333.07 -0.45	16	17	02.41	-50	31	22.1	-55.0
333.16 -0.10	16	15	55.41	-50	12	41.1	-93.0
333.20 -0.08	16	16	00.12	-50	10	08.1	-83.0
333.24 +0.05	16	15	38.20	-50	02	39.1	-60.0
333.45 -0.18	16	17	32.01	-50	04	08.1	58.1
335.55 -0.31	16	27	11.30	-48	39	28.0	-116.0
335.73 +0.19	16	25	46.00	-48	11	23.0	-44.0
336.07 -1.08	16	32	47.01	-48	48	34.1	-75.0
336.36 -0.14	16	29	47.90	-47	57	28.1	-73.0
336.50 -0.15	16	30	23.11	-47	52	23.1	-100.0
336.51 -1.48	16	36	21.01	-48	44	57.6	-23.7
336.74 +0.13	16	30	11.21	-47	29	39.1	-76.0
336.83 +0.02	16	31	00.60	-47	30	20.1	-77.0
336.86 +0.01	16	31	11.21	-47	29	39.1	-76.0
336.96 -0.12	16	32	09.60	-47	30	27.6	-120.0
336.99 -0.03	16	31	53.00	-47	25	08.1	-120.0
337.12 -0.17	16	33	02.01	-47	25	18.0	-76.8
337.61 -0.06	15	34	29.10	-46	59	17.0	-48.0
337.63 -0.08	16	34	38.70	-46	58	53.1	-57.0
337.71 -0.04	16	34	47.00	-46	54	13.1	-47.0
337.86 +0.26	16	34	04.01	-46	34	54.1	-86.0
337.94 -0.42	16	37	20.81	-46	58	45.0	-38.7
337.97 +0.14	16	35	01.31	-46	35	18.1	-41.0
337.99 +0.14	16	35	07.01	-46	34	11.1	-38.0
338.07 +0.02	16	35	58.21	-46	35	28.1	19.0
338.09 +0.01	16	36	03.01	-46	35	16.0	-47.0
338.27 +0.54	16	34	28.70	-46	05	19.0	-60.0
338.45 +0.06	16	37	13.61	-46	16	54.2	-40.0
338.46 -0.25	16	38	36.11	-46	28	38.0	-50.0
338.47 +0.29	16	36	19.21	-46	06	50.0	-44.0
338.68 -0.08	16	38	44.21	-46	12	09.0	-23.0
338.87 -0.08	16	39	28.71	-46	03	38.0	-41.0
338.93 -0.06	16	39	36.51	-46	00	05.0	-42.0

Table 2 – *continued*

Source (l, b)		RA (1950) h	m	s	Dec (1950) °	′	″	LSR radial velocity[a] (km s⁻¹)
339.63	-0.13	16	42	30.01	-45	31	22.0	-36.0
339.68	-1.21	16	47	25.01	-46	10	59.0	-21.0
340.06	-0.25	16	44	39.01	-45	16	26.1	-55.0
340.28	-0.22	16	45	20.00	-45	05	21.0	-43.0
340.79	-0.10	16	46	38.36	-44	37	18.5	-110.0
340.80	-1.02	16	50	41.00	-45	12	18.0	-27.0
341.28	+0.06	16	47	43.91	-44	08	41.0	-74.0
342.01	+0.25	16	49	31.01	-43	27	40.0	-43.9
342.09	+0.42	16	49	03.81	-43	17	30.0	-65.0
343.93	+0.12	16	56	38.71	-42	02	58.0	14.0
344.21	-0.59	17	00	38.01	-42	16	00.0	-20.0
344.42	+0.05	16	58	37.11	-41	42	36.0	-71.0
344.44	+0.05	16	58	40.20	-41	41	44.8	-15.0
344.58	-0.02	16	59	27.01	-41	37	38.0	-5.5
345.65	+0.01	17	02	45.61	-40	45	56.0	-8.7
345.69	-0.09	17	03	18.01	-40	47	22.0	-9.0
347.64	+0.16	17	08	23.00	-39	05	09.0	-84.0
348.72	-1.04	17	16	39.01	-38	54	36.0	-12.8
350.02	+0.43	17	14	23.81	-36	59	53.0	-30.0
351.20	+0.64	17	16	58.01	-35	54	48.0	-6.5
351.62	+0.17	17	20	01.31	-35	50	30.0	-43.0
352.01	-0.49	17	23	48.51	-35	53	17.0	-20.0
353.29	-2.42	17	35	15.40	-35	53	17.0	-50.0
355.34	+0.15	17	30	12.01	-32	45	54.0	15.0
356.64	-0.33	17	35	26.01	-31	55	60.0	-10.0
358.26	-2.04	17	46	18.00	-31	27	60.0	9.0
359.14	+0.03	17	40	14.60	-29	38	12.0	2.5
359.43	-0.10	17	41	28.30	-29	27	04.0	-49.0
359.83	-17.84	18	58	17.11	-37	06	49.9	0.0
359.91	-17.85	18	58	29.40	-37	02	48.9	0.0
1.53	-23.97	19	30	05.01	-37	37	23.9	0.0
1.57	-0.02	17	46	15.00	-27	34	60.0	54.8
1.71	-23.82	19	29	35.01	-37	25	11.9	0.0
2.14	+0.01	17	47	29.00	-27	05	01.0	59.0
3.91	-0.01	17	51	35.60	-25	34	19.0	2.0
6.69	-0.30	17	58	49.80	-23	19	27.0	11.3
8.38	-47.14	21	29	20.99	-36	04	41.8	0.0
8.99	-46.52	21	26	22.99	-35	37	41.8	0.0
9.62	+0.20	18	03	15.98	-20	31	52.9	1.3
10.39	-46.63	21	27	17.00	-34	40	41.8	0.0
10.48	-47.12	21	29	40.99	-34	39	11.8	0.0
11.91	-0.15	18	09	18.10	-18	42	24.9	42.0
11.93	-0.62	18	11	04.70	-18	54	29.0	0.0
12.03	-0.04	18	09	07.40	-18	32	39.0	108.0
12.21	-0.11	18	09	45.00	-18	25	09.9	23.0
17.64	+0.15	18	19	37.30	-13	31	45.0	21.0
18.46	-0.01	18	21	47.99	-12	53	02.0	48.0
19.48	+0.16	18	23	10.30	-11	54	31.0	21.0
20.24	+0.08	18	24	55.80	-11	16	24.0	72.0
22.44	-0.18	18	30	01.00	-09	26	60.0	31.0
24.33	+0.11	18	32	32.30	-07	38	24.0	113.0
27.18	-0.08	18	38	32.29	-05	11	60.0	19.5
27.35	-0.20	18	39	16.00	-05	06	35.0	12.0
28.21	-0.05	18	40	21.60	-04	16	26.0	100.0
28.83	-0.25	18	42	12.40	-03	49	08.0	86.0
30.22	-0.15	18	44	24.00	-02	31	60.0	108.0
30.82	+0.27	18	44	00.50	-01	48	29.0	95.0

Notes: (a) The velocity coverage of the spectrometer is $+54$ km s^{-1}, centred on the velocity given here. (b) Heliocentric velocity.

separate components in the spectrum; there is an H_2O maser (Cesaroni et al. 1988) at this position, but no 6.7-GHz emission has been reported.

23.43−0.19. This source shows a complex profile at 44 GHz, with four narrow features and one broad feature (Fig. 41). Menten (1991b) found a 6.7-GHz maser with spectral features in the same radial velocity interval.

4.2 Properties of the 44-GHz masers

Almost all sources detected in the present survey have linewidths <1 km s^{-1} and some are as narrow as 0.2 km s^{-1}. The exceptions are several quasi-thermal sources, mentioned in Section 4.1, which have linewidths from 0.7 to 2 km s^{-1}. The sources for which a grid of points was observed were unresolved with our beam, again with the exception of one quasi-thermal source. Combined with a rather high flux density, this is strong evidence for most of the new 44-GHz methanol sources being masers. More conclusive evidence for maser action in these sources must await interferometric measurements of their angular size.

4.3 Relation to other masers

This survey was not made over the whole Galactic plane but was directed to known H II regions, H_2O and OH masers, as well as previously detected methanol masers at 6.7- and 12-GHz methanol absorption sources. It is not surprising, therefore, that most of the new 44-GHz sources were found at the position of previously known masers. Over 80 per cent of the new 44-GHz sources are associated with H_2O or OH masers. What is more interesting is that 82 per cent of the new 44-GHz sources were found at the positions of 6.7-GHz methanol masers. This fraction may indeed be higher, as many of the remaining sources have not been observed at 6.7 GHz. A somewhat lower percentage (64 per cent) of 44-GHz methanol masers detected in the Northern Hemisphere surveys are associated with 6.7-GHz masers. More observations at 6.7 GHz are clearly needed to determine the extent of the 6.7- and 44-GHz correlation.

4.4 Class I–Class II connection

The 44-GHz masers belong to Class I methanol masers (Menten 1991a), and the 6.7-GHz masers belong to Class II. The difference between the two classes is that each of them has its own set of methanol transitions and its own set of sources. However, while the separation of methanol transitions into two classes is straightforward, and probably corresponds to different maser pumping mechanisms, the association of Class I and II masers with different sets of astronomical objects is more ambiguous. There are examples of pure Class I sources like NGC 2264, in which there is a strong emission at 44 GHz, and absorption instead of emission at 6.7 GHz. An example of a pure Class II source is CepA, with very strong emission at 6.7 GHz and no emission at 44 GHz (Haschick et al. 1990; Menten 1991b). However, as previous surveys suggested and present results show, most of the sources are mixed Class I–Class II emitters and share the same volume on a large scale together with H_2O and OH masers. The statistics show that there are more 6.7-GHz (Class II) masers than 44-GHz (Class I) masers, but almost all of the Class I masers have a 6.7-GHz counterpart. This is not true for Class II masers, many of which have no associated Class I masers. When both Class I and II masers are observed at the same position, the spectra of the two masers are invariably different. Although the spectral features occupy a common radial velocity interval, there is no one-to-one correspondence of the spectra. Rather, there is a tendency for spectral features of one class to avoid positions in radial velocity occupied by spectral features of the other class. The evidence for this is further supported by the inverse correlation of flux densities between the two classes in the same source. If the flux density of 6.7-GHz emission is high, the corresponding 44-GHz emission is weak, and *vice versa*. In our survey the sources at 44 GHz with flux densities greater than 100 Jy corresponded to sources at 6.7 GHz which were, on average, a factor 0.32[1] weaker; however, for sources at 6.7 GHz with flux density >100 Jy, the corresponding 44-GHz emission is weaker by a factor of 21[2]. This means that strong 6.7-GHz emission suppresses that at 44 GHz, and *vice versa*. In extreme cases of very strong masers the suppression is complete, resulting in pure Class I or Class II masers like NGC 2264 and CepA. A similar tendency was found for the sources of northern surveys, where the corresponding flux ratios are 0.32 and 15.

A natural explanation for this can be understood in the model where masers of both classes share the same volume filled with the submillimetre radiation field pumping Class II masers (Cragg et al. 1992). This radiation field is producing population inversion in Class II transitions, but may reduce or even destroy population inversion, which is produced by collisions, in Class I transitions (Lees 1973). The stronger the radiation field, the more intensive the Class II masers become, and the dimmer the Class I masers. If the radiation field is weak or absent, Class II masers disappear and Class I masers gain their full power. Weak Class I and Class II masers may co-exist in the same region without much interference. This finding is incompatible with Menten's (1991a; cf. Batrla et al. 1987) definition of Class I and Class II methanol masers, based on the type of associated astronomical object. We suggest that Class I and Class II masers should be defined as those emitting in one or other set of methanol transitions.

5 CONCLUSIONS

As a result of a comprehensive survey of the southern sky with the Parkes radio telescope at 44 GHz, 55 new methanol sources were detected, almost the same number as detected in the Northern Hemisphere surveys. Most of the new sources are associated with OH and/or H_2O masers, as well as with 6.7-GHz methanol masers. Evidence for the anti-correlation between fluxes at 44 and 6.7 GHz was found, indicating that both masers occupy the same volume in space, despite the assignment of the two methanol transitions to different classes. Thus the definition of Class I and II masers should be modified, since the difference is mainly in different sets of methanol transitions.

[1]The ratio of the mean 6.7-GHz flux density to the mean 44-GHz flux for the set of sources with 44-GHz flux density above 100 Jy.
[2]The ratio of the mean 6.7-GHz flux to the mean 44-GHz flux for the set of sources with 6.7-GHz flux above 100 Jy. For the sources with upper limit at 44 GHz, the flux density was assumed to be equal to 1/2 of the upper limit.

ACKNOWLEDGMENTS

This project was made possible by support from the Australian Department of Industry, Technology and Regional Development under the Russia–Australia Bi-Lateral Science and Technology Agreement, and by the special efforts of Dr D. L. Jauncey and Professor R. D. Ekers. We acknowledge the staff of the Parkes Observatory for the excellent performance of the Q-band receiver (G. Moorey, G. Gay and M. Sinclair), assistance with observations (E. Troup and H. Fagg) and for their hospitality. We thank Dr J. L. Caswell for giving us an unpublished list of the southern 6.7-GHz masers, Ms H. May and Drs L. Staveley-Smith and T. Oosterloo for their help in data reduction, and Ms D. Goddard for help in preparing the manuscript. Observations were carried out and this paper written during the stay of VIS, SVK and IEV̄ at the ATNF, Australia. This work was partially supported by the Russian Foundation for Fundamental Research.

REFERENCES

Bachiller R., Menten K. M., Gomez-Gonzalez J., Barcia A., 1990, A&A, 240, 116

Batchelor R. A., Caswell J. L., Goss W. M., Haynes R. F., Knowles S. H., Wellington K. J., 1980, Aust. J. Phys., 33, 139

Batrla W., Matthews, H. E., Menten K. M., Walmsley C. M., 1987, Nat, 326, 49

Caswell J. L., Haynes R. F., Goss W. M., 1980, Aust. J. Phys., 33, 639

Cesaroni R., Palagi F., Felli M., Catarzi M., Comoretto G. D., Di Franco S., Giovanardi C., Palla F., 1988, A&AS, 76, 445

Cragg D. M., Johns K. P., Godfrey P. D., Brown R. D., 1992, MNRAS, 259, 203

Forster J. R., Caswell J. L., Okumura S. K., Hasegawa T., Ishiguro M., 1990, A&A, 231, 473

Haschick A. D., Menten K. M., Baan W. A., 1990, ApJ, 354, 556

Haynes R. F., Caswell J. L., Simons L. W. J., 1978, Aust. J. Phys., Astrophys. Suppl. no. 45, 1

Kalenskii S. V., Bachiller R., Berulis I. I., Val'tts I. E., Gomez-Gonzalez J., Martin-Pintado J., Rodrigez-Franco A., Slysh V. I., 1992, AZh, 64, 1002

Kalenskii S. V., Berulis I. I., Val'tts I. I., Dzura A. M., Slysh V. I., Vasil'kov V. I., 1993, AZh, in press

Lada C. J., Gull T. R., Gottlieb C. A., Gottlieb E. W., 1976, ApJ, 203, 159

Lees R. M., 1973, ApJ, 184, 763

MacLeod G. C., Gaylard M. J., 1992, MNRAS, 256, 519

MacLeod G. C., Gaylard M. J., Nicolson G. D., 1992, MNRAS, 254, 1P

Menten K. M., 1991a, in Haschick A. D., Ho P. T. P., eds, Skylines, Proc. 3rd Haystack Observatory Meeting. Astron. Soc. Pac., San Francisco, p. 119

Menten K. M., 1991b, ApJ, 380, L75

Moore C. R., Neff D., 1982, IEEE Trans. Microw. Theory Tech., 30, 2013

Morimoto M., Ohishi M., Kanzawa T., 1985, ApJ, 288, L11

Peng R. S., Whiteoak J. B., 1992, MNRAS, 254, 301